Inorganic Chemistry

Article

pubs.acs.org/IC

Observation of the Sixth Polymorph of BiB_3O_6: In Situ High-Pressure Raman Spectroscopy and Synchrotron X-ray Diffraction Studies on the β-Polymorph

Rihong Cong,[†,‡] Tao Yang,*[,†] Junliang Sun,[‡] Yingxia Wang,[‡] and Jianhua Lin*[,‡]

[†]College of Chemistry and Chemical Engineering, Chongqing University, Chongqing 400044, People's Republic of China

[‡]Beijing National Laboratory for Molecular Sciences, State Key Laboratory of Rare Earth Materials Chemistry and Applications, College of Chemistry and Molecular Engineering, Peking University, Beijing 100871, People's Republic of China

Supporting Information

ABSTRACT: β-BiB_3O_6 was compressed in a diamond anvil cell at room temperature and studied using a combinstion of in situ high-pressure Raman scattering and angle-dispersive synchrotron X-ray diffraction. The results reveal that β-BiB_3O_6 retains its structure below 9.0 GPa and undergoes a structural phase transition that starts at ~11.5 GPa and finishes at ~18.5 GPa. No other phase transition occurred with increasing pressure up to ~46 GPa. It was also found that the high-pressure phase is different from the already-reported five polymorphs of BiB_3O_6. Therefore, the new phase is denoted as ζ-BiB_3O_6, which could be indexed by an orthorhombic unit cell ($a \approx 12.5$ Å, $b \approx 6.7$ Å, $c \approx 4.0$ Å) from the powder XRD pattern collected at 22.2 GPa. Moreover, ζ-BiB_3O_6 can be quenched to ambient conditions. The investigation of the pressure dependence of the lattice parameters reveals that both β-BiB_3O_6 and ζ-BiB_3O_6 exhibit a large amount of crystallographic anisotropy. An unusual expansion of the c-axis of ζ-BiB_3O_6 was observed. Assignments for the Raman spectra of β-BiB_3O_6, γ-BiB_3O_6, and δ-BiB_3O_6 under ambient conditions were also performed. Currently, we cannot solve the crystal structure of ζ-BiB_3O_6 but give some speculations based on its relationship with β-BiB_3O_6.

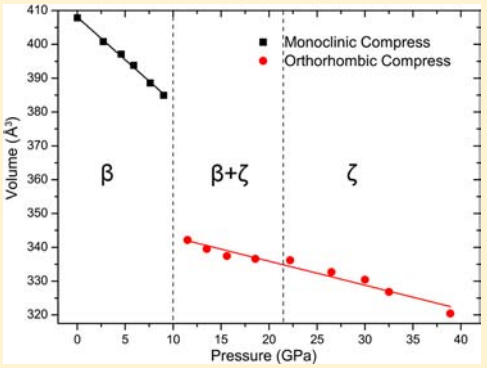

INTRODUCTION

The phase diagram of the Bi_2O_3–B_2O_3 system under equilibrium conditions has been well-investigated since 1962.[1] Five compounds were found, including $Bi_{24}B_2O_{39}$, $Bi_4B_2O_9$, $Bi_3B_5O_{12}$, BiB_3O_6, and $Bi_2B_8O_{15}$. Recent interest in this system is related to the outstanding nonlinear optical (NLO) properties of BiB_3O_6, which possess a polar structure and has been demonstrated as one of the most promising NLO materials with an optical birefringence of $\Delta n \approx 0.09$ and an effective SHG coefficient of $d_{eff} \approx 3.2$ pm/V.[2−8] It crystallizes in the monoclinic space group $C2$ and contains borate layers with a BO_4/BO_3 ratio of 1/2.[2,3] Theoretical calculation based on the first principles revealed that the NLO coefficients originate mainly from the $(BiO_4)^{5-}$ group.[7]

Four more modifications of BiB_3O_6 were identified.[9−11] Li et al. synthesized β- and γ-BiB_3O_6 by employing boric acid flux method in sealed containers.[9] β-BiB_3O_6 contains borate layers, which can be depicted as an inner-layer condensation of α-BiB_3O_6, resulting in a BO_4/BO_3 ratio of 2/1. The borate network in γ-BiB_3O_6 is three-dimensional (3D) and is constructed exclusively of BO_4 units. Li et al. claimed that the borate framework in γ-BiB_3O_6 can be expressed as interlayer condensation of the borate layers in β-BiB_3O_6. However, both β-BiB_3O_6 and γ-BiB_3O_6 crystallize in the centrosymmetric space group $P2_1/n$. δ-BiB_3O_6 was synthesized by applying the multianvil high-pressure technique at 5.5 GPa and 820 °C.[10] δ-BiB_3O_6 contains a 3D borate framework constructed exclusively of BO_4 units, and interestingly, it crystallizes in the orthorhombic space group $Pca2_1$, similar to that of the widely used NLO crystal LiB_3O_5. The fifth modification of ε-BiB_3O_6 can only be stabilized at elevated pressures starting from α-BiB_3O_6 at room temperature.[11] The phase transition from α-BiB_3O_6 to ε-BiB_3O_6 is first-order and occurs at pressures between $P = 6.09$ GPa and $P = 6.86$ GPa. The problem is that ε-BiB_3O_6 cannot be quenched. After releasing the pressure, α-BiB_3O_6 is recovered.

With regard to the technological importance of α-BiB_3O_6, it is desirable to learn the chemistry behind these polymorphs. Therefore, remarkable studies were performed on the stability, crystal growth, physical properties, and phase relationship of the BiB_3O_6 polymorphs.[2−7,9−16] A previous study on α-BiB_3O_6 using variable-temperature neutron and X-ray diffraction (XRD) techniques on powder and single-crystalline samples revealed the anisotropic thermal behavior of this phase, but did not find any evidence of structural phase transformation to other polymorphs between 3.5 K and 999 K at ambient pressure.[12] Recently, a detailed investigation of the phase

Received: February 1, 2013
Published: June 14, 2013

   dx.doi.org/10.1021/ic400268p | Inorg. Chem. 2013, 52, 7460−7466

transitions among the α-, β-, γ-, and δ-phases under different temperatures and pressures was reported.[13] From the structural point of view, the dimensionality of the borate framework increases from two-dimensional (2D) in the α- and β-phases to 3D in the γ- and δ-phases, and the BO_4/BO_3 ratio also shows a similar increasing tendency. Therefore, the phase transitions between these four polymorphs must involve a considerable B−O bond breaking and reformation; consequently, long-time annealing treatments and a seed-induced technique were applied, which indeed overcome the kinetic effect successfully.[13] Phase transitions of $\beta \rightarrow \alpha \rightarrow \delta \rightarrow \gamma$ and $\alpha/\beta \rightarrow \gamma \rightarrow \delta$ were observed under high-temperature/ambient-pressure conditions and high-temperature/high-pressure conditions, respectively.[13]

Thermodynamic relationships between BiB_3O_6 polymorphs provide guidance for the synthesis and crystal growth of specified modifications.[13,14,16] The phase relationship of α-, γ-, and δ-phases, which are all thermodynamically stable under certain conditions, was expressed in a pressure−temperature (P−T) phase diagram.[13] At ambient pressure, α-BiB_3O_6 is the high-temperature phase and is stable in a narrow temperature range of 710−715 °C, while γ-BiB_3O_6 is stable in the intermediate temperature range of 680−710 °C. In addition, the high-pressure phase of δ-BiB_3O_6 is stable below 670 °C at ambient pressure, and the stability field extends as the pressure increases. To date, all three of the thermodynamically stable phases—α-, γ- and δ-BiB_3O_6—were grown as bulk crystals, using the top-seeded method at atmospheric pressure.[4−6,14,16] The measurements of the NLO coefficients on the δ-BiB_3O_6 single crystal revealed that the largest d_{33} value is 2.4 ± 0.4 pm/V, which is of the same order of magnitude as that of α-BiB_3O_6,[15] and the transmission spectrum of the single crystal of γ-BiB_3O_6 was recorded in a polarized light beam.[16]

In contrast to α-, γ-, and δ-BiB_3O_6, β-BiB_3O_6 is somewhat special, because of its metastability. The motivation of our current study is to utilize its metastable characteristics to prepare new polymorphs under moderate conditions (i.e., high pressure at room temperature). A combination of in situ Raman spectroscopy and angle-dispersive synchrotron X-ray powder diffraction (XRD) measurements were performed, using a diamond-anvil cell (DAC). A careful analysis of the results suggests a high-pressure phase transition, which leads to the sixth polymorph, ζ-BiB_3O_6. Moreover, measurements and assignments for the Raman spectra of β-, γ-, and δ-BiB_3O_6 under ambient conditions were performed.

EXPERIMENTAL SECTION

β-BiB_3O_6 was prepared by the boric acid flux method in a sealed container. Typically, a mixture of 0.5 g of Bi_2O_3 (1.07 mmol) and 3.32 g of H_3BO_3 (53.7 mmol) was ground and put into a 50-mL Teflon container, and 0.4 mL of distilled water was added. The container was further sealed in a steel vessel and kept at 240−260 °C statically for 3−7 days in an oven, and then cooled to room temperature. The product was extensively washed with warm distilled water (50 °C), to remove the residual boric acid, and dried at 80 °C. The obtained β-BiB_3O_6 is transparent with colorless platelet-like single crystals.

The Raman spectra of the powder samples of α-, β-, γ-, and δ-BiB_3O_6 were collected at room temperature and atmospheric pressure by using a Nicolet Raman 950 spectrometric analyzer with a resolution of ~1 cm^{-1}. A near-infrared (NIR) laser beam with a wavelength of 1064 cm^{-1} from an YVO_4:Nd^{3+} laser source was used for excitation.

Pressure was generated by using an improved Mao-Bell-type DAC with 500-μm diamond culets. T301 stainless steel preindented up to 10 GPa with a thickness of 50 μm was used as the gasket, where a small hole, 200 μm in diameter, was drilled as the sample chamber. An appropriate amount of β-BiB_3O_6, which was ground in an agate mortar, and a few grains of ruby used for pressure calibrating were carefully loaded into the chamber. In order to obtain a hydrostatic pressure condition, a mixture of methanol and ethanol with a molar ratio of 4:1 was applied as the pressure transmitting medium. The pressure was determined from the frequency shift of the ruby $R1$ fluorescence line.[17] By monitoring the separation and widths of both the $R1$ and $R2$ lines, we confirmed that hydrostatic conditions were maintained throughout these experiments. The precision in our pressure measurements was estimated to be ~0.05 GPa.

Room-temperature Raman spectroscopic measurements were performed by using a LABRAM-HR confocal laser micro-Raman spectrometer (HR800) equipped with a charge-coupled device detector in backscattering geometry. Raman spectra at different pressures were collected in the frequency range from 50 cm^{-1} to 1200 cm^{-1}. The 532-nm line of the Verdi-2 solid-state laser was used as a Raman excitation source. A 25× microscope objective lens was applied to focus the laser beam and collect the scattered light.

In situ high-pressure XRD experiments were carried out with a DAC at room temperature on the 3W1A high-pressure beamline at the Beijing Synchrotron Radiation Facility (BSRF). The pressure was measured off-line by the ruby line shift method.[17] Diffraction patterns were recorded with a fixed radiation wavelength in an angle-dispersive mode. The spot size and wavelength of the X-ray were 20 μm × 60 μm and 0.62014 Å, respectively. The diffraction patterns were collected by a Marresearch Model MAR345 online image-plate detector as a 2D Debye−Scherrer diffraction image. The *FIT2D* program was used to convert the 2D diffraction image to a conventional one-dimensional (1D) angle-resolved XRD pattern by intergrading images as a function of 2θ.[18]

RESULTS AND DISCUSSION

Ambient Pressure Raman Spectroscopy for α-, β-, γ-, and δ-BiB_3O_6. Raman spectroscopy is a convenient technique to study structural characteristics through the solid-state effects on the dynamical properties. Until now, many bismuth-containing borate structures have been investigated by Raman, infrared (IR) spectroscopy, and XRD analyses.[19−21] The vibrational spectra of α-BiB_3O_6 have been studied several times;[22−24] however, the Raman spectra of β-, γ-, and δ-BiB_3O_6 under ambient conditions have not been reported. For comparison, we measured the spectrum of α-BiB_3O_6 in the range of 50−1200 cm^{-1} (see Figure 1). The Raman spectrum of ε-BiB_3O_6 crystals was not obtained, because of its instability

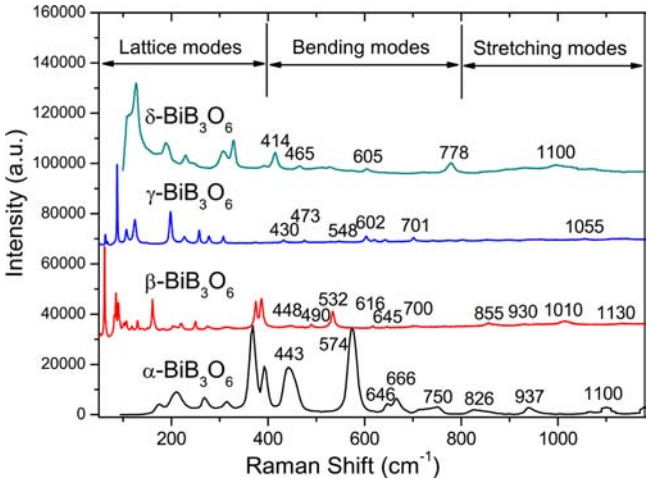

Figure 1. Raman spectra of α-, β-, γ-, and δ-BiB_3O_6 under ambient conditions.

dx.doi.org/10.1021/ic400268p | Inorg. Chem. 2013, 52, 7460−7466

under ambient conditions. It is known that the vibrational spectra of bismuth borates are determined by vibrations of Bi−O and B−O structural units.[19,22,23] The following frequency ranges have been proposed for the BiB_3O_6 system: the vibrational bands below 400 cm^{-1} can be assigned as lattice modes, including external vibration of Bi atoms (50−150 cm^{-1}), internal vibrations along the Bi−O bonds, translational and vibrational motions of BO_3 and BO_4 groups (150−400 cm^{-1}).

As shown in Figure 1, the intensities of observed lattice modes are strong for β-, γ-, and δ-BiB_3O_6. The bending vibrations of the BO_3 and BO_4 groups occur in a broad range (400−800 cm^{-1}).[22,23] It is known that only BO_4 groups exist in γ- and δ-BiB_3O_6,[9,10] so it is reasonable that all these vibrations in the range of 400−800 cm^{-1} can be assigned to the bending vibrations of BO_4 groups.

According to the assignment results of α-BiB_3O_6 in literature,[22−24] we interpret the spectrum of β-BiB_3O_6 as below. Two weak modes at 645 and 700 cm^{-1} are assigned to bending vibrations of BO_3 groups, and the other modes in the range 400−800 cm^{-1} are from bending vibrations of BO_4 groups. The stretching vibrations of BO_3 and BO_4 groups appear in the 800−1500 cm^{-1} range.[19,22,23] Generally, vibrations occurring in the range 740−890 cm^{-1} and 1000−1150 cm^{-1} are assigned to the BO_4 symmetric (ν_s) and asymmetric stretching vibrations (ν_{as}), respectively; for BO_3, the frequencies of ν_s and ν_{as} lie in the range of 850−960 cm^{-1} and 1100−1450 cm^{-1}, respectively.[19] Therefore, the mode positioned at 930 cm^{-1} was assigned to the ν_s of BO_3; the remaining modes centered at ∼855, 1010, and 1130 cm^{-1} were assigned to the ν_s and ν_{as} vibrations of BO_3 or BO_4, respectively.

In Situ High-Pressure Raman Spectroscopy for β-BiB_3O_6. With the development of DAC technique, high-pressure Raman spectroscopy has become available to investigate pressure-related structural characteristics.[25,26] For the first time, we present a pressure-dependent Raman scattering study to detect the structural behavior of β-BiB_3O_6. All of the Raman spectra in various pressures up to 46 GPa were shown in Figure 2. The pressure shifts of the observed Raman peaks are summarized and plotted in Figure 3. As analyzed for the Raman spectra of BiB_3O_6 polymorphs under ambient conditions, the Raman peaks under different pressures are assigned in three frequency regions: 50−400 cm^{-1}, 400−800 cm^{-1}, and 800−1200 cm^{-1}, corresponding to the lattice modes, bending modes, and stretching modes of borate groups, respectively.

According to position shift and change of intensity with increasing pressure in the pressure range of 10^{-5}−5.8 GPa (Figure 2), it is clear that the peaks in the regions of 400−800 cm^{-1} and 800−1200 cm^{-1} are more sensitive to pressure than those peaks in the region of 50−400 cm^{-1}. The positions of the peaks in the region of 50−200 cm^{-1} are almost unchanged. The upward shift in the range of 200−400 cm^{-1} is relatively recognizable (0.73−2.08 cm^{-1}/GPa). The intensities of most peaks decrease when the pressure increases. Moreover, upon the continuous enhancement of pressure from ambient to 5.8 GPa, the broadening of the Raman peaks and the merging of several adjacent modes are remarkable. It can be easily recognized that the two peaks at ∼200 cm^{-1} and the two peaks at ∼375 cm^{-1} almost merge at 5.8 GPa. As mentioned above, the peaks in the range of 50−150 cm^{-1} mainly correspond to external vibrations of Bi atoms; the remaining peaks are related to the borate groups. Therefore, these observations indicate that the pressure effect is less sensitive for external vibrations of Bi atoms than the vibrations of borate groups.

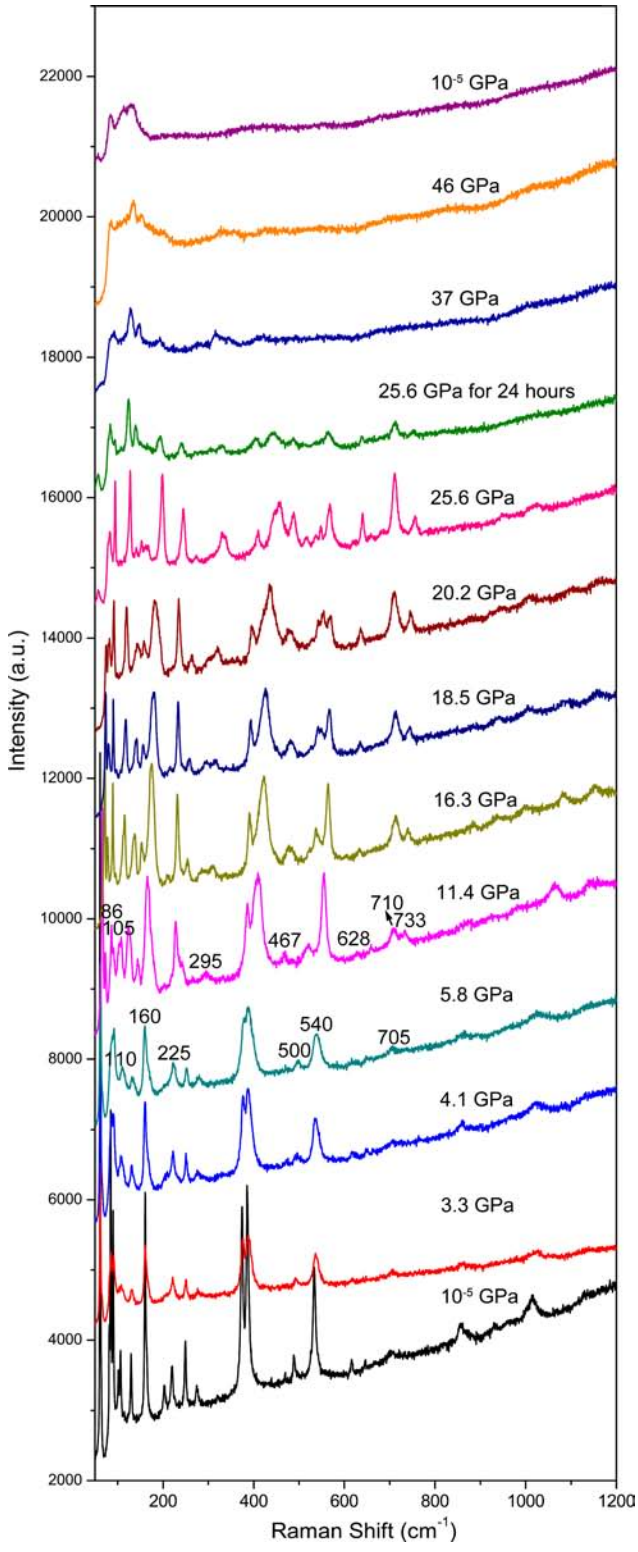

Figure 2. Raman spectra of β-BiB_3O_6 at different pressures (intensities are manually shifted for better presentation).

When the pressure reaches 11.4 GPa, several new Raman peaks appear, as shown in Figures 2 and 3. The intensities of some peaks are enhanced suddenly from 5.8 GPa to 11.4 GPa,

dx.doi.org/10.1021/ic400268p | Inorg. Chem. 2013, 52, 7460−7466

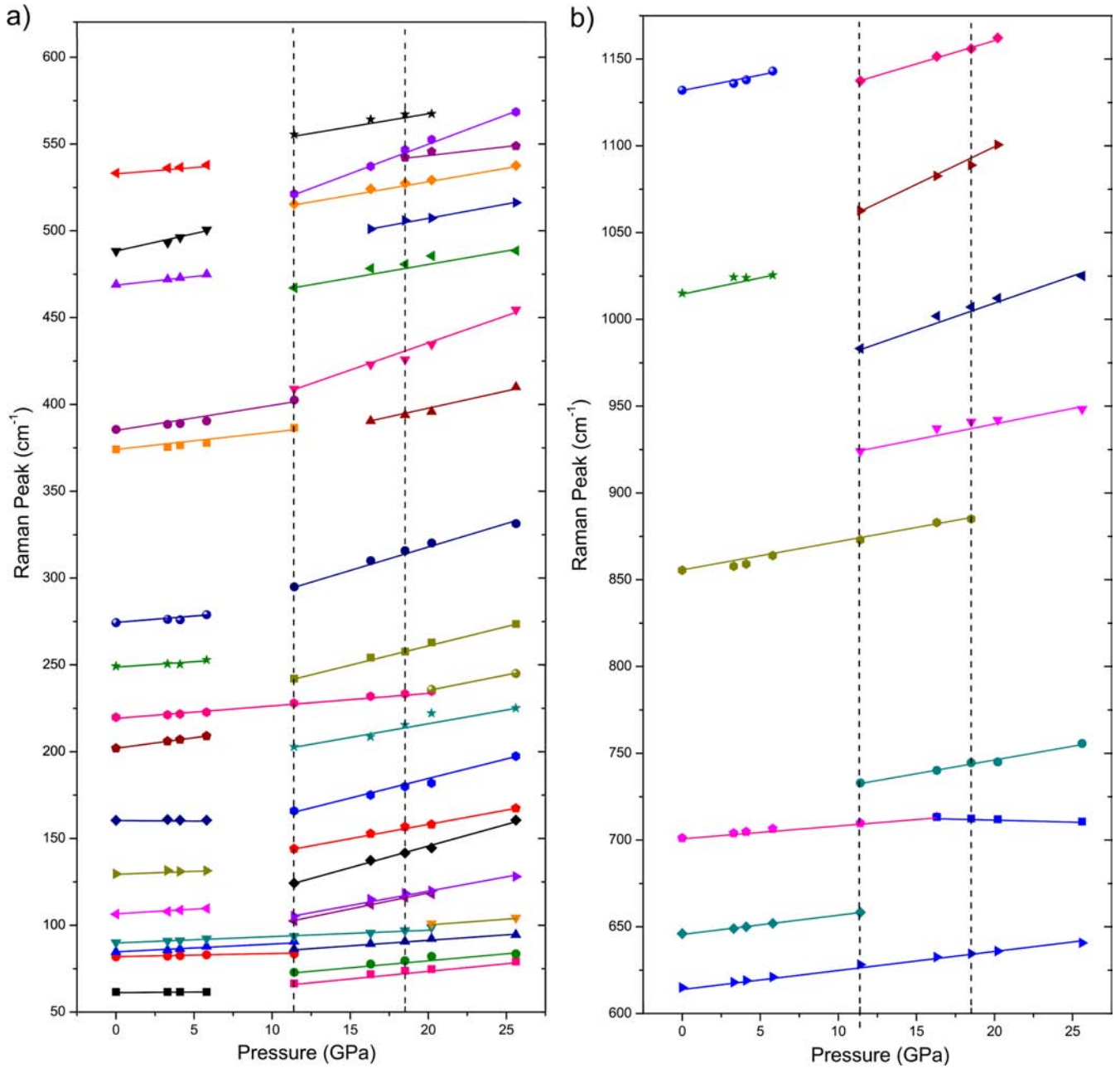

Figure 3. Pressure-dependent shifts of the observed Raman peaks under compression: (a) 50−600 cm^{-1} and (b) 600−1175 cm^{-1}.

such as the peaks near 110, 160, 225, 500, 540, and 705 cm^{-1} (marked in Figure 2). Moreover, new peaks obviously grow as the pressure increases from 11.4 GPa to 25.6 GPa. These can be readily recognized as peaks appearing at ∼86, 105, 295, 467, 628, 710, and 733 cm^{-1}. It should be noted that the peak-shifting rates in the pressure range of 11.4−25.6 GPa (0.59−4.12 cm^{-1}/GPa) are generally larger than those below 5.8 GPa. In other words, there are apparent discontinuities at ∼5.8 and 11.4 GPa on most of the modes, as shown in Figure 3. All these observations suggest a pressure-induced phase transition starting from ∼11.4 GPa, and two different crystal structures that coexist in the intermediate pressure range (11.4−18.5 GPa). One is the parent phase, β-BiB_3O_6, and the other is the new high-pressure phase, defined as ζ-BiB_3O_6. From the Raman spectra and XRD analyses (discussed below), ζ-BiB_3O_6 is distinguished from all five polymorphs of BiB_3O_6 observed hitherto.

The content of ζ-BiB_3O_6 in the sample increases with increasing pressure, and all the Raman peaks of β-BiB_3O_6 disappear at 20.2 GPa. With pressures up to 25.6 GPa, no other new Raman peak can be distinguished. Keeping the pressure at 25.6 GPa for 24 h, the peaks of ζ-BiB_3O_6 become broadening. Upon a continuous enhancement of pressure to 46 GPa, the peaks becomes more broadening, but the major characteristic is maintained. It is understandable that the crystallization becomes worse at ultrahigh pressures, because no further phase transition occurs. After the pressure is released, the peaks of the high-pressure structure mostly remained, although the crystallization of the sample is very poor.

In summary, three pressure regions were distinguished by Raman experiments: region I, 10^{-5}−5.8 GPa; region II, 11.4−

dx.doi.org/10.1021/ic400268p | Inorg. Chem. 2013, 52, 7460−7466

18.5 GPa; and region III, above 20.2 GPa. In region I, only β-BiB_3O_6 exists. These modes related to borate groups are more sensitive to pressure than those corresponding to Bi atoms. This was illustrated by the shift rate of frequencies of Raman peaks. In region II, ζ-BiB_3O_6 emerges and coexists with β-BiB_3O_6. In region III, β-BiB_3O_6 phase completely disappears and only the peaks of ζ-BiB_3O_6 are observed in the spectra. With further increases in pressure, the crystallization of ζ-BiB_3O_6 becomes worse. Finally, the high-pressure phase remains after the pressure is released.

In Situ High-Pressure X-ray Diffraction for β-BiB_3O_6. Raman spectroscopy studies cannot give more information about the structural details. Therefore, in situ XRD experiments at different pressures up to 38.9 GPa were performed (see Figure 4). For better understanding, the pressure dependence

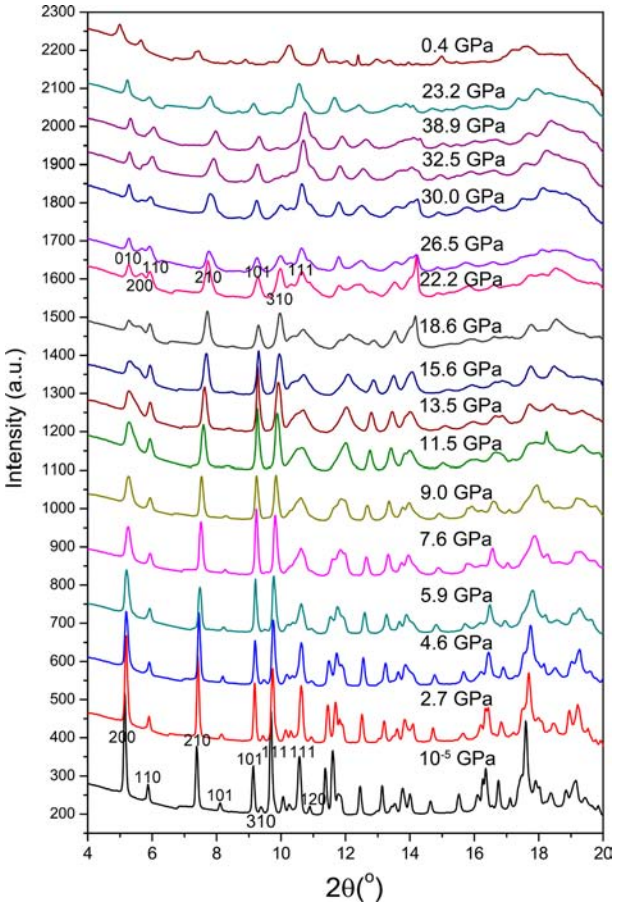

Figure 4. In situ XRD patterns at different pressures (λ = 0.62014 Å; intensities have been manually shifted for better presentation).

of diffraction peaks is also plotted in Figure S1 in the Supporting Information. Like the Raman experiments, three pressure regions with different characteristics were observed. In the first region of 10^{-5}–9.0 GPa, the XRD patterns shows a continuous change, indicated by peak shifting toward higher angles. Le Bail fitting was applied on the first 6 patterns using the lattice parameters of β-BiB_3O_6 as shown in Figure 6a and Figure S2 in the Supporting Information. The good convergence of the Le Bail fitting confirmed that only β-BiB_3O_6 existed. The change of the lattice parameters will be discussed later.

In the second region of 11.5–18.6 GPa, the (200) peak splits to two peaks with increasing pressure, and the peaks in the range of 10.0°–10.8°, 11.0°–12.0°, 13.5°–14.5°, 16.0°–16.5°, 17.0°–18.2°, 18.5–19.5° become overlapped and ultimately merge. The discontinuous changes in the XRD patterns, particularly the disappearing of the peaks of β-BiB_3O_6 and the growing of new peaks, point to a pressure-induced phase transformation from β-BiB_3O_6 to ζ-BiB_3O_6. In this pressure range, two phases coexist. The angular positions of the main reflections do not change much during the phase transition, so similar unit-cell parameters and volumes could be also expected for ζ-BiB_3O_6. It is similar to the case of the phase transition from α- to ε-BiB_3O_6.[11]

In the last region of 22.2–38.9 GPa, β-BiB_3O_6 completely disappears and only the peaks of ζ-BiB_3O_6 are present. The possible lattice parameters of ζ-BiB_3O_6 were obtained from the pattern at 22.2 GPa using *PowderX*:[28] orthorhombic, $a \approx 12.5$ Å, $b \approx 6.7$ Å, $c \approx 4.0$ Å. The peak profiles and lattice parameters at pressure from 11.5 GPa to 38.9 GPa were refined using Le Bail fitting. As representatives, the fitting of XRD patterns at 15.6, 22.2, and 32.5 GPa are shown in Figures 6b–6d. The original diffraction rings recorded by the image plate were also presented. Numerous strong reflection dots are observed at relatively low pressures, showing the good crystalline of the sample. At highest pressure, the crystallinity of the sample dramatically decreases. No further structural details, like the exact space group and atomic coordinates, were resolved because of the broadening and thus serious overlapping of the XRD peaks at such high pressure. The XRD pattern of ζ-BiB_3O_6 is different from that of α-, β-, γ-, and δ-BiB_3O_6 (see Figure S3 in the Supporting Material) and ε-BiB_3O_6 (in ref 11). Moreover, it is also not similar to any other bismuth borates ($Bi_{24}B_2O_{39}$, $Bi_4B_2O_9$, $Bi_3B_5O_{12}$, and $Bi_2B_8O_{15}$) or bismuth oxides. Thus one can conclude that here we observe a pressure-induced phase transition from β- to ζ-BiB_3O_6, an unprecedented polymorph of BiB_3O_6.

No further discontinuous changes were observed in the XRD patterns (Figure 4) with increasing pressure, up to the highest pressure: 38.9 GPa. After the pressure was released, the structure of ζ-BiB_3O_6 could be quenched under ambient conditions, which is also consistent with the Raman experiments.

Note that an amorphous tendency was observed in Raman measurements, because the sample was kept for 24 h under 25.6 GPa during Raman measurements, and no similar process was applied during XRD.

Crystal Structure Relationship between β-BiB_3O_6 and ζ-BiB_3O_6. Generally, the normalized lattice parameters at elevated pressures for β- and ζ-BiB_3O_6 show linearity (see Figure 6). The crystal structure of β-BiB_3O_6 is highly compressible and is stable up to 9.0 GPa (Figure 6a). As shown in Figure S4 in the Supporting Information, the structure of β-BiB_3O_6 is built of alternating Bi atoms and borate layers along the a-axis, where the BO_3/BO_4 ratio is 1:2.[9] Bi^{3+} are irregularly coordinated by seven oxygen atoms (Bi–O bond distance = 215–278 pm). As shown in Figure 6a, increasing the pressure to 9.0 GPa results in a faster decrease in parameter a than the respective changes in b, c, and β. Such a crystallographic anisotropy is similar to that of α-BiB_3O_6,[11,12] from which one can expect a higher compressibility along the layer stacking direction (the b-axis in α-BiB_3O_6, but the a-axis in β-BiB_3O_6).

dx.doi.org/10.1021/ic400268p | Inorg. Chem. 2013, 52, 7460–7466

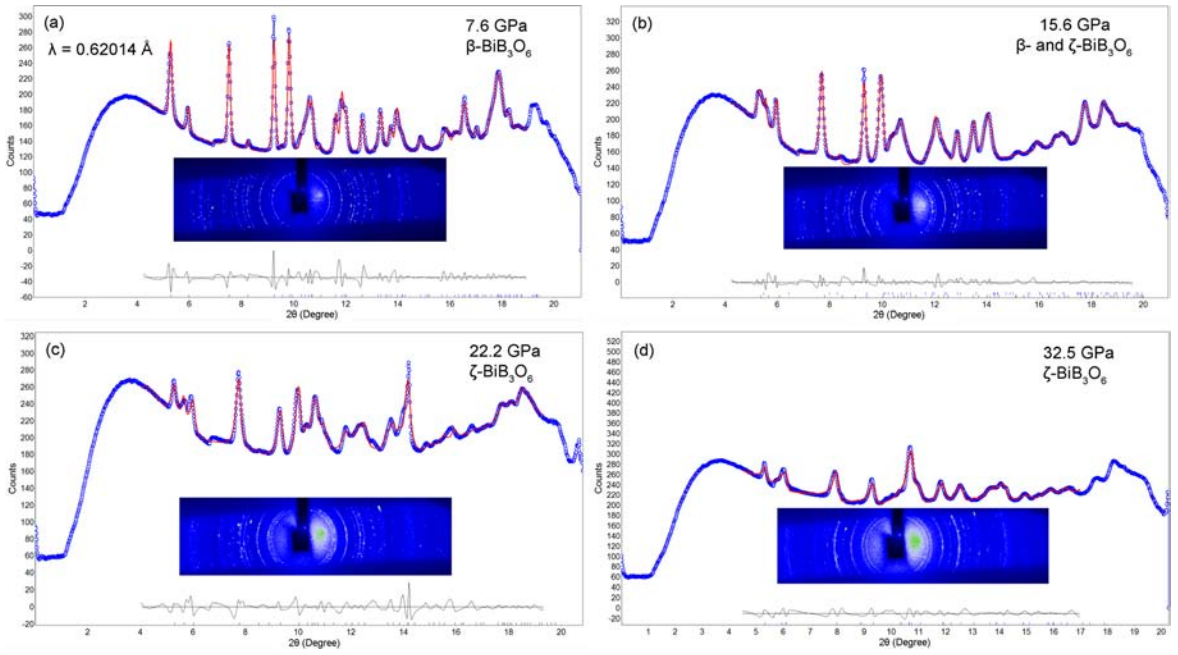

Figure 5. Le Bail fittings of the in situ high-pressure synchrotron XRD patterns for β-BiB_3O_6 (only part of the patterns was refined) using TOPAS.[27] The circles (○) represent the observed data, and the red solid line is the calculated pattern. The marks below the diffraction patterns are the expected reflection positions; the difference curve (shown in gray) is also shown below the diffraction curves.

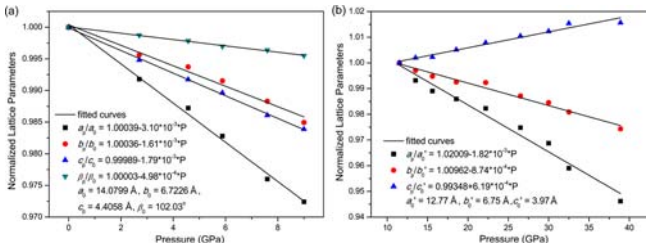

Figure 6. Room-temperature normalized lattice parameters-pressure plots for β-BiB_3O_6 and ζ-BiB_3O_6.

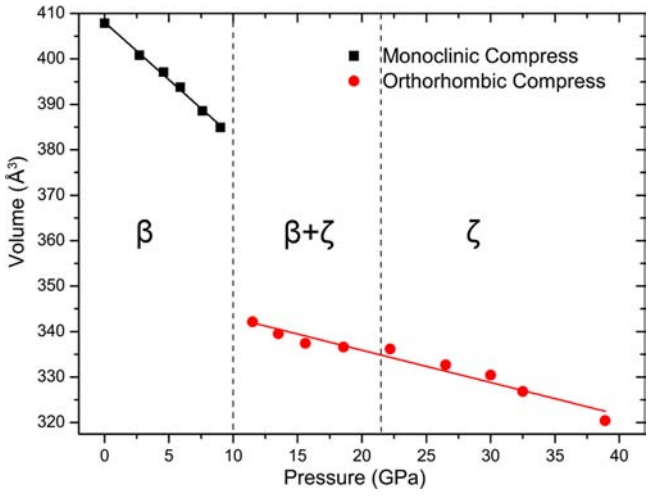

Figure 7. Room-temperature cell volume−pressure plots for β-BiB_3O_6 and ζ-BiB_3O_6.

Starting at a pressure of 11.5 GPa, β-BiB_3O_6 exhibits a first-order phase transition to ζ-BiB_3O_6. The possible orthorhombic cell lattice is obtained via auto indexing, using *PowderX*:[28]. Again, the *a*-axis is more sensitive with pressure than the *b*- and *c*-axes (see Figure 6b), which means the structure of ζ-BiB_3O_6 is probably still two-dimensional. As shown in Figure 7, the *V*−*P* curve shows an obvious discontinuity between 9.0 GPa and 11.5 GPa, i.e., an ∼8% decrease in volume at 11.5 GPa. We need to point out that the compressibilities for the transition from β-BiB_3O_6 to γ-BiB_3O_6 and for the transition from β-BiB_3O_6 to δ-BiB_3O_6 are 12 vol % and 15 vol %, respectively.[13] The β-BiB_3O_6 to ζ-BiB_3O_6 transition occurs under milder conditions than the β-BiB_3O_6 to γ-BiB_3O_6 transition and the β-BiB_3O_6 to δ-BiB_3O_6 transition (for example, 0.85 GPa/490 °C or 0.4 GPa/600 °C). Apparently, the simultaneous high-pressure and high-temperature conditions are crucial to realize the β- to γ- and δ-BiB_3O_6 transitions, which involve covalent bonds breakings and reformations. Then, it is expected that structure change during the β-BiB_3O_6 to ζ-BiB_3O_6 transition is insignificant. Thus, the proposed cell lattice for ζ-BiB_3O_6 is logical.

The easy compressibility in the layer-stacking direction in β-BiB_3O_6 and ζ-BiB_3O_6 also suggests the structural similarity of these two polymorphs. The unusual expansibility of the *c*-axis in ζ-BiB_3O_6 by observing the left-shifts of the XRD peaks, which are nonzero for *l* (such as 011, 411, 501, and 511; see Figure S1 in the Supporting Information), indicates that what happens at this critical pressure is a phase transition rather than a decomposition. Similar behavior was observed for α-BiB_3O_6,[11] where the *a*-axis also expands as the pressure increases. The observed strong anisotropy in the *bc*- and *ab*-planes for α- and ζ-BiB_3O_6, respectively, can both be attributed to a "Nuremberg scissors effect" within the borate layers.[11]

In the literature,[13] the α- to ε-BiB_3O_6 transition at room temperature is mainly characterized by a reorientation of the BO_3 triangles, the BO_4 tetrahedra, and the lone electron pair of Bi^{3+}.[11] Herein, the β-BiB_3O_6 to ζ-BiB_3O_6 phase transition is likely to involve only the reorientation of the borate groups and the higher coordination number of Bi^{3+} ions, not the breaking or (re)formation of B−O bonds. However, we have failed to

dx.doi.org/10.1021/ic400268p | Inorg. Chem. 2013, 52, 7460−7466

propose a reasonable structure model, because of the poor XRD quality under high-pressure conditions (see Figure S5 in the Supporting Information).

CONCLUSION

A pressure-induced phase transition from β-BiB_3O_6 to a new polymorph, ζ-BiB_3O_6, has been identified by the combination of in situ Raman spectroscopy and synchrotron X-ray diffractions. Pressure dependence of the Raman and XRD peaks suggested that there existed three pressure regions related to different structural characters. First, β-BiB_3O_6 remains stable up to a pressure of 9.0 GPa; second, ζ-BiB_3O_6 emerges at 11.5 GPa and coexists with β-BiB_3O_6 until 18.5 GPa; third, β-BiB_3O_6 completely transfers to ζ-BiB_3O_6 above 20.2 GPa. This phase transition is irreversible. By analyzing the XRD patterns, we observed large crystallographic anisotropy for both β-BiB_3O_6 and ζ-BiB_3O_6. Interestingly, an unusual expansion of the *c*-axis of ζ-BiB_3O_6 upon compression was observed, which is similar to the case of α-BiB_3O_6. The poor quality of the XRD data under high pressure hampers determination of the structure of ζ-BiB_3O_6. Referring to the little changes of the structure during the α- to ε-BiB_3O_6 phase transition, we speculate that ζ-BiB_3O_6 may possess a layered structure similar to β-BiB_3O_6. Considering the technical importance of bismuth-containing borates, especially BiB_3O_6, our work gives a new window to obtain new polymorphs of BiB_3O_6, starting with the metastable β-BiB_3O_6.

ASSOCIATED CONTENT

Supporting Information

Le Bail fitting of the powder XRD pattern for β-BiB_3O_6 below 9 GPa; pressure dependence of the XRD peaks at different regions; XRD patterns (Cu Kα radiation) at room temperature for α-, β-, γ-, and δ-BiB_3O_6; structure views of β-BiB_3O_6. This material is available free of charge via the Internet at http://pubs.acs.org.

AUTHOR INFORMATION

Corresponding Author

*Tel.: +86-23-65105065 (T.Y.), +86-10-62751715 (J.L.). E-mail addresses: jhlin@pku.edu.cn (J.L.), taoyang@cqu.edu.cn (T.Y.).

Notes

The authors declare no competing financial interest.

ACKNOWLEDGMENTS

This work was supported by the Nature Science Foundation of China (NSFC NOs. 21101175, 21171178, 91222106). We acknowledge the help from Changqing Jin (Institute of Physics, Chinese Academy of Sciences) for the physical measurements.

REFERENCES

(1) Levin, E. M.; McDaniel, C. L. *J. Am. Ceram. Soc.* **1962**, *45*, 355–360.
(2) Liebertz, J. *Z. Kristallogr.* **1982**, *158*, 319.
(3) Fröhlich, R.; Bohatý, L.; Liebertz, J. *Acta Crystallogr., Sect. C: Cryst. Struct. Commun.* **1984**, *40*, 343–344.
(4) Becker, P.; Liebertz, J.; Bohatý, L. *J. Cryst. Growth* **1999**, *203*, 149–155.
(5) Teng, B.; Wang, J. Y.; Wang, Z. P.; Hu, X. B.; Jiang, H. D.; Liu, H.; Cheng, X. F.; Dong, S. M.; Liu, Y. G.; Shao, Z. S. *J. Cryst. Growth* **2001**, *233*, 282–286.
(6) Hellwig, H.; Liebertz, J.; Bohatý, L. *Solid State Commum.* **1999**, *109*, 249–251.
(7) Lin, Z. S.; Wang, Z. Z.; Chen, C. T.; Lee, M. H. *J. Appl. Phys.* **2001**, *90*, 5585–5590.
(8) Yang, J.; Dolg, M. *J. Phys. Chem. B* **2006**, *110*, 19254–19263.
(9) Li, L. Y.; Li, G. B.; Wang, Y. X.; Liao, F. H.; Lin, J. H. *Inorg. Chem.* **2005**, *44*, 8243–8248.
(10) Knyrim, J. S.; Becker, P.; Johrendt, D.; Huppertz, H. *Angew. Chem., Int. Ed.* **2006**, *45*, 8239–8241.
(11) Dinnebier, R. E.; Hinrichsen, B.; Lennie, A.; Jansen, M. *Acta Crystallogr., Sect. B: STruct. Sci.* **2009**, *65*, 1–10.
(12) Stein, W. D.; Cousson, A.; Becker, P.; Bohatý, L.; Braden, M. *Z. Kristallogr.* **2007**, *222*, 680–689.
(13) Cong, R. H.; Zhu, J. L.; Wang, Y. X.; Yang, T.; Liao, F. H.; Jin, C. Q.; Lin, J. H. *CrystEngComm* **2009**, *11*, 1971–1978.
(14) Aleksandrovsky, A. S.; Vasiliev, A. D.; Zaitsev, A. I.; Zamkov, A. V. *J. Cryst. Growth* **2008**, *310*, 4027–4030.
(15) Cherepakhin, A. V.; Zaitsev, A. I.; Aleksandrovsky, A. S.; Zamkov, A. V. *Opt. Mater.* **2012**, *34*, 790–792.
(16) Gavryushkin, P. N.; Isaenko, L. I.; Yelisseyev, A. P.; Gets, V. A.; Il'ina, O. S. *Cryst. Growth Des.* **2012**, *12*, 75–78.
(17) Mao, H. K.; Xu, J. A.; Bell, P. M. *J. Geophys. Res.* **1986**, *191*, 4673–4676.
(18) Hammersley, A. P.; Svensson, S. O.; Hanfland, M.; Fitch, A. N.; Hausermann, D. *High Press. Res.* **1996**, *14*, 235–248.
(19) Egorysheva, A. V.; Burkov, V. I.; Kargin, Yu. F.; Plotnichenko, V. G.; Koltashev, V. V. *Crystallogr. Rep.* **2005**, *50*, 127–136.
(20) Weir, C. E.; Schroeder, R. A. *J. Res. Natl. Bur. Stand., Sect. A* **1964**, *68*, 465.
(21) Egorysheva, A. V.; Kanishcheva, A. S.; Kargin, Yu. F.; Gorbunova, Yu. E.; Mikhailov, Yu. N. *Russ. J. Inorg. Chem.* **2002**, *47*, 1804–1808.
(22) Kaminskii, A. A.; Becker, P.; Bohatý, L.; Ueda, K.; Takaichi, K.; Hanuza, J.; Maczka, M.; Eichler, H. J.; Gad, G. M. A. *Opt. Commun.* **2002**, *206*, 179–191.
(23) Kasprowicz, D.; Runka, T.; Szybowicz, M.; Ziobrowski, P.; Majchrowski, A.; Michalski, E.; Drozdowski, M. *Cryst. Res. Technol.* **2005**, *40*, 459–465.
(24) Hu, X. B.; Wang, J. Y.; Teng, B.; Loong, C. K.; Grimsditch, M. *J. Appl. Phys.* **2005**, *97*, 033501.
(25) Pravica, M. G.; Shen, Y. R.; Nicol, M. F. *Appl. Phys. Lett.* **2004**, *84*, 2452.
(26) Long, Y. W.; Zhang, W. W.; Yang, L. X.; Yu, Y.; Yu, R. C.; Ding, S.; Liu, Y. L.; Jin, C. Q. *Appl. Phys. Lett.* **2005**, *87*, 181901.
(27) *TOPAS, V4.1-beta*, Bruker AXS, Karlsruhe, Germany, 2004.
(28) Dong, C.; Wu, F.; Chen, H. *J. Appl. Crystallogr.* **1999**, *32*, 850.